Eur. Phys. J. E **16**, 253–258 (2005)
DOI 10.1140/epje/i2004-10080-6

THE EUROPEAN PHYSICAL JOURNAL E

Evidence of the hexagonal columnar liquid-crystal phase of hard colloidal platelets by high-resolution SAXS

D. van der Beek, A.V. Petukhov, S.M. Oversteegen, G.J. Vroege, and H.N.W. Lekkerkerker[a]

Van 't Hoff Laboratory for Physical and Colloid Chemistry, Utrecht University Padualaan 8, 3584 CH Utrecht, The Netherlands

Received 4 August 2004 and Received in final form 14 October 2004 /
Published online: 20 January 2005 –

Abstract. We report Small-Angle X-ray Scattering (SAXS) measurements of the columnar phase of hard colloidal gibbsite platelets. We have been able to create large oriented domains of the columnar phase both perpendicular and parallel to the sample wall, varying the volume fraction of platelets and adding non-adsorbing polymer to the dispersion. In conjunction with the increased resolution of the SAXS setup, this allowed a detailed analysis of the columnar phase, providing unambiguous evidence for the hexagonal nature of the phase.

PACS. 61.10.-i X-ray diffraction and scattering – 61.30.-v Liquid crystals – 82.70.-y Disperse systems; complex fluids

1 Introduction

Colloidal suspensions that form periodic self-assembling structures on sub-micrometre scales are of potential technological interest. For instance, three-dimensional arrangements of spheres in colloidal crystals [1] might serve as photonic materials [2–4], intended to manipulate light. Colloidal particles with non-spherical shapes (such as rods and plates) are of particular interest because of their ability to form liquid crystals that might serve as templates for ordered porous materials.

It has long been known that dispersions of anisotropic colloids display liquid-crystal phases. The earliest reports date back to the 1920s and 1930s, when suspensions of rod- and platelike colloids were found to exhibit the isotropic (I) to nematic (N) phase transition. For rodlike colloids, the I-N transition was found to occur in suspensions of vanadium pentoxide (V_2O_5) ribbons [5] and tobacco mosaic virus (TMV) rods [6]. Already in the 1940s, Lars Onsager proposed an explanation for the I-N transition on a purely entropic basis [7]: the competition between packing entropy (which favours the nematic state) and orientational entropy (favouring the isotropic state) determines the I-N phase behaviour. As the packing entropy becomes more important at higher volume fractions, the particles tend to align and form a nematic phase at high enough concentration. Onsager also showed that the particle shape alone is enough to induce such behaviour. Moreover, at a later stage, it was found that rodlike colloids show the nematic–to–smectic-A phase transition, as in the case of TMV [8,9], fd virus [10–12] and β-FeOOH [13]. A detailed description of this phase transition came with theory [14–18] and computer simulations [19,20], showing that hard-core interactions are enough to induce such ordering.

As stated, platelike particles also exhibit the I-N transition. The first ever observation of this kind was done by Langmuir [21], who reported in 1938 on sols of California bentonite clay particles that, after standing for several 100 hours, separated into two distinct phases —the isotropic and nematic phase. During the last decades, there have been quite a few studies on natural and synthetic clays, investigating their phase behaviour [22–26], rheological [27–29] and structural properties [30–33]. However, in almost all of the studies, clay suspensions were found to gel rather than phase separate (I-N), as was the case with Langmuir's sample. Model systems of colloidal platelets that do show the I-N transition have recently become available [34, 35], confirming both Onsager's theory and computer simulations [36]. From computer simulations by Veerman and Frenkel [37], and later Zhang *et al.* [38], it was found that hard platelets may also form another liquid-crystal phase, namely the orientationally and 2D translationally ordered columnar (C) phase. This phase has also been observed experimentally in suspensions of sterically stabilised and charged colloidal plates [39–41]. There is a very interesting issue, raised in one of these reports [39], which is related to the inherent size polydispersity in these synthetic suspensions: it is quite surprising that such systems, with a rather high polydispersity of up to 25%, show the columnar liquid-crystal phase. In contrast, crystallisation of hard spheres is suspected to be frustrated due to the so-called terminal polydispersity, with proposed values from 5% to 12% [42–46].

[a] e-mail: h.n.w.lekkerkerker@chem.uu.nl

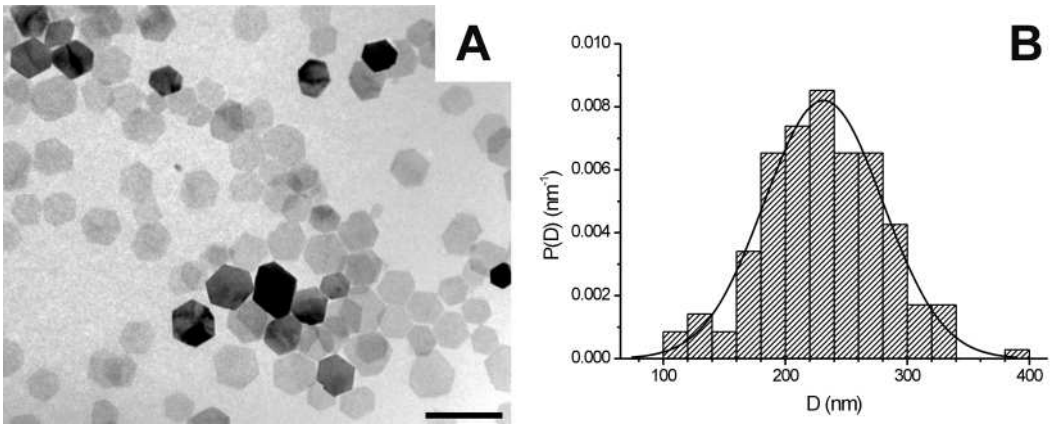

Fig. 1. Panel A shows a Transmission Electron Micrograph of the colloidal gibbsite platelets; the scale bar denotes 500 nm. Panel B depicts the normalised diameter distribution of the colloidal gibbsite platelets used in this study, together with a Gaussian fit. From the fit, we obtain $\langle D \rangle = 232$ nm and $\sigma = 20\%$, based on 176 platelets measured.

Nevertheless, on the basis of their Small-Angle X-ray Scattering (SAXS) data, van der Kooij *et al.* [39] argue that the observed high-density liquid-crystal phase is most likely a hexagonal columnar phase. Their argument for a hexagonal packing of the columns is founded on the observation of three low-angle scattering peaks within the powder pattern. However, they noted the absence of a fourth low-angle peak that should also be present in the scattering pattern of a hexagonal structure. Conclusive evidence would require sufficiently large monodomains with columns perpendicular to the sample wall, revealing scattering patterns with sixfold symmetry corresponding to hexagonal packing. Usually, oriented samples are prepared by applying an external field, *e.g.* magnetic fields [47–51] and shear flow [52–54]. Here, we use sterically stabilised colloidal gibbsite platelets with non-adsorbing polymer as a depleting agent. We have been able to successfully prepare large crystals of hard colloidal *spheres* for SAXS studies [55,56] using such non-adsorbing polymer before. In addition, in the case of platelets, the depletion interaction is expected to favour a perpendicular orientation of the columns with respect to the sample walls. Moreover, we took advantage of the enhanced resolution of the SAXS setup [57] in order to resolve the missing scattering peak. Our results show that we indeed could prepare large oriented domains of columnar phase, allowing us to demonstrate its hexagonal columnar nature.

2 Experimental section

We synthesised hexagonal colloidal gibbsite ($Al(OH)_3$) platelets [58] that were subsequently grafted with an end-functionalised polyisobutene and suspended in toluene to obtain a model system of hard platelets [34,39]. Transmission Electron Microscopy (TEM, see Fig. 1A) and Atomic Force Microscopy (AFM) were used to determine the average corner-to-corner diameter, D, and thickness, L, of the dry particle core, although the latter might contain a contribution of the collapsed steric stabiliser. The diameter distribution is shown in Figure 1B. We found $\langle D \rangle = 232$ nm and $\langle L \rangle = 13$ nm and a polydispersity of $\sigma = 20\%$ in both dimensions. In solution the thickness of the sterically stabilizing polyisobutene brush is estimated as 2–3 nm. This gives us the effective dimensions $D_{\rm eff} = 237$ nm and $L_{\rm eff} = 18$ nm.

Table 1. Details of the samples used in this study. Here, age is the time between sample preparation and measurements of the SAXS patterns, ϕ denotes the volume fraction of the platelets and $c_{\rm pol}$ is the polymer concentration.

Sample	age (d)	ϕ	$c_{\rm pol}$ (g/l)
A	16	0.40	0.0
B	8	0.37	0.0
C	3	0.37	0.8

We prepared several samples of this dispersion with effective volume fractions ranging from 0.37 to 0.40 both with and without non-adsorbing polymer (polydimethylsiloxane, $M_{\rm w} \approx 423$ kDa and $R_{\rm g} \approx 33$ nm [59]). The samples were thoroughly homogenised and subsequently put in flat capillaries (internal dimensions 0.3×3.0 mm^2), after which they were put away to phase separate. Within a few days, phase separation was complete and yielded multiple phase equilibria [59]. Each sample at least exhibited nematic and columnar phases. Furthermore, Bragg reflections became visible, already hinting at the presence of a columnar phase. On a timescale of months, these colours got quite bright and distinct, see Figure 2, although we were not able to detect a change in the colour. The reflections allowed us to get an estimate of the hexagonal lattice spacing $d_{(100)} = 220 \pm 15$ nm using Bragg's law.

From the set of samples, three representative samples (hereafter called A, B, and C) were selected for analysis with SAXS. The sample details are given in Table 1. We used the recently developed [57] high-resolution SAXS setup of the Dutch-Belgian beamline BM-26 DUBBLE at the European Synchrotron Radiation Facility (ESRF, Grenoble, France). One of the challenges in the application of SAXS to our suspensions of colloidal platelets is related to the existence of two distinctly different spatial scales.

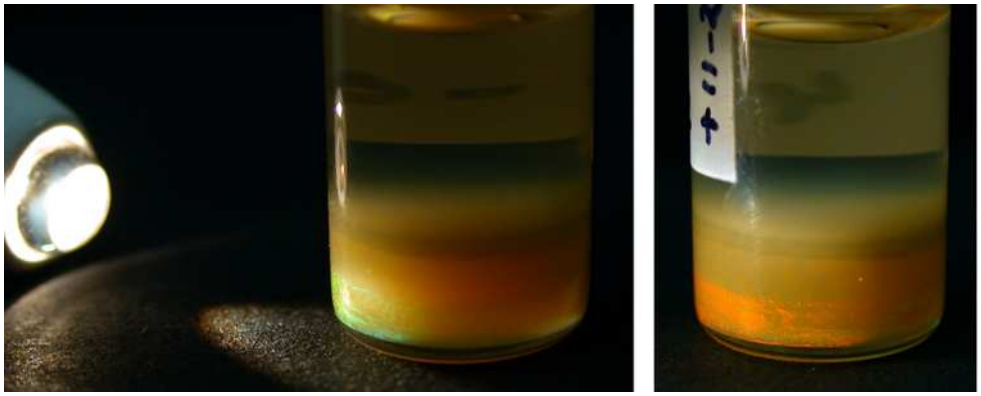

Fig. 2. Bragg reflections from the columnar phase of a sample with experimental conditions comparable to the ones in this study (platelets and non-adsorbing polymer). The colour of the reflections (cyan and red) varies with the incident angle. These Bragg reflections already hint at the presence of a columnar structure, and allow a crude estimate of the inter-columnar spacing.

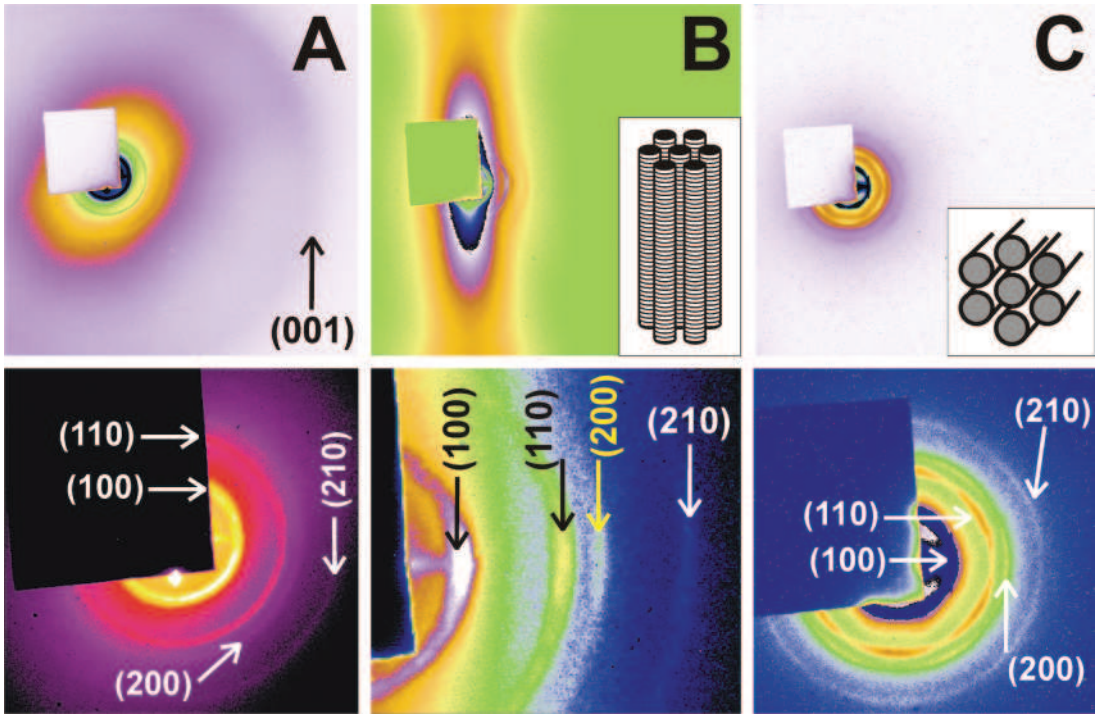

Fig. 3. SAXS patterns obtained in the columnar phase of samples A, B and C, along with the assigned Miller indices. The upper panels depict the entire SAXS patterns, while the lower panels present the magnified views of the small scattering angle regions near the beamstop. Sample A yields ringlike diffraction features typical for diffraction from a powder. In contrast, samples B and C show strong predominant orientation of the columns, either along the vertical direction (in B) or along the X-ray beam (in C), as shown by the inserted sketches. The hexagonal pattern in C points to the presence of the hexagonal columnar phase.

Due to the small particle thickness, the face-to-face interparticle structure leads to scattering at relatively large angles. On the other hand, due to the relatively large particle diameter, the side-to-side structure results in scattering at very small angles, requiring a high reciprocal-space resolution. To achieve the latter, the X-ray beam was carefully focused at the position of the X-ray detector consisting of a phosphor screen coupled to a 16-bit CCD camera (Photonic Science) with a pixel size of 22 μm. In order to increase the maximum accessible q-range, a relatively high X-ray energy of 18 keV ($\lambda = 0.69$ Å) and a shorter sample-detector distance (about 5 m) were used. In addition, the detector and beamstop were mounted off-centre to maximise the q-range even further. These settings allowed us to achieve a resolution of 0.003 nm^{-1} (the full-width at half maximum of the instrument function), which is at least 3 times higher than before [39]. The smallest accessible scattering angle corresponded to $q_{\rm min} = 0.023$ nm^{-1}. The maximum q values were about $q_{\rm max,h} = 0.4$ nm^{-1} in the horizontal plane and $q_{\rm max,v} = 0.24$ nm^{-1} in the vertical direction.

3 Results and discussion

Figure 3 displays the obtained SAXS patterns for samples A to C. In the following we will index the reflections using Miller indices (hkl). For a hexagonal packing we expect reflections perpendicular to the columns with $q_{(hk0)}$ proportional to $\sqrt{h^2+hk+k^2}$, while we use l to indicate (liquidlike) order within the columns. Sample A shows the characteristics expected for a columnar phase, *i.e.*, four scattering peaks with q-ratios of $1{:}\sqrt{3}{:}\sqrt{4}{:}\sqrt{7}$ at small angles and a much broader, liquidlike peak at large angle. The small-angle inter-columnar peaks have an apparent width of 0.003 nm^{-1}, determined by the instrument's resolution. The large-angle intra-columnar peak has a width of order of 0.07 nm^{-1}. The ringlike features are typical for diffraction from a powder, hence, the domains of columnar phase must be much smaller than the irradiated volume ($300 \times 300 \times 300$ $\mu\mathrm{m}^3$). We attribute the small domains to the relatively high volume fraction that causes fast crystallisation yielding small crystallites [1]. Sample B shows the columnar scattering peaks more clearly than sample A. In this case the scattering is dominated by a larger single domain, likely due to slower crystallisation and higher mobility at the lower volume fraction involved. The domain has vertically oriented columns, as illustrated in the inset in panel B. The liquidlike (001) and (00−1) peaks are located outside the detector area, but they were visible in similar samples with skewed orientations. In sample C we find a single domain with columns directed perpendicularly to the wall and we observe a hexagonal scattering pattern due to inter-columnar scattering. Here the presence of non-adsorbing polymer is found to favour the face-to-wall anchoring of the gibbsite platelets, which can be understood by the stronger depletion attraction in this configuration. We also note that in the azimuthal direction the inter-columnar Bragg peaks are broad, of the order of 30°, suggesting a significant spread of the crystal orientations.

From the SAXS patterns, we calculated averaged radial intensity profiles that are depicted in Figure 4. Due to the improved resolution of the SAXS setup, the inter-columnar (100), (110), (200) and (210) reflections are clearly resolved. Yet, we are not able to resolve the intrinsic width of the Bragg peaks. In addition, in samples B and C we benefit from the predominant orientation of the columnar domains that enhances the visibility of the inter-columnar reflections. This is due to an increase of the intensity of the reflections themselves and to a faster decay of the background scattering intensity I_{sc} at q values from $q_{(100)}$ to $q_{(001)}$. The behaviour of the background can be understood by taking into account the anisotropy of the scattering of a single particle, *i.e.*, the form factor $F(\boldsymbol{q})$. For disklike particles it can be factorised as $F(\boldsymbol{q}) = F_n(q_n) \times F_{||}(\boldsymbol{q}_{||})$, where q_n and $\boldsymbol{q}_{||}$ are the components of the scattering vector perpendicular and parallel to the disk, respectively. In the q-range of interest (from $q_{(100)}$ to $q_{(001)}$) the first factor $F_n(q_n)$ does not decay appreciably, while the second one decays as $F_{||}(\boldsymbol{q}_{||}) \propto |\boldsymbol{q}_{||}|^{-3}$. Thus, the strongest scattering is observed for small $q_{||}$, when the scattering vector $\boldsymbol{q}$ is nearly orthogonal to the platelets. In sample C this strong contribution is absent since the scattering vector $\boldsymbol{q}$ is almost parallel to the platelets, so $q \approx q_{||}$. As one can see in Figure 4, the background intensity indeed closely follows a power law decay $I_{\mathrm{sc}}(q) \propto q^n$ with exponent $n = -3$, arising from the decay of $F_{||}$. In contrast, in sample A, the particles have all possible orientations including those with $q \approx q_n$, which give the main contribution to the background. Averaging over all possible orientations leads to a power law decay with a smaller exponent, $n = -2$. We have observed a similar power law decay with $n = -2$ in a dilute isotropic suspension (not shown). In sample B, both phenomena are visible —the background scattering intensity along the columns (perpendicular to the platelets, vertical direction) is much stronger and decays more slowly than when parallel to the platelets (horizontal direction).

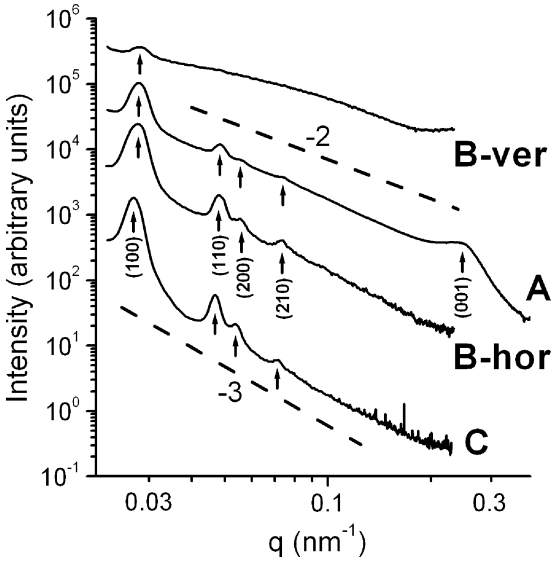

Fig. 4. Averaged radial intensity profiles of the SAXS patterns. The profiles of sample B were obtained from small (about 5 pixel wide) horizontal (B-hor) and vertical (B-ver) slices, while A and C are azimuthal averages over the whole available detector area except for the part covered by the beamstop (the same mask is used for both A and C). The curves are shifted vertically for clarity. The dashed lines present the power law decays ($I \propto q^n$) with $n = -2$ and $n = -3$.

We further note that, although the diffraction in sample B is dominated by a domain with vertically oriented columns, other orientations are also present, as deduced from the observation that the columnar reflections form rings, albeit with well-pronounced maxima in the horizontal direction. Also, the maxima of the (100), (110), and (210) reflections in the same direction suggest a spread in the orientations of the hexagons formed by neighbouring columns. In contrast, sample C shows long-range bond orientational order leading to a well-pronounced hexagonal pattern. Furthermore, the q^{-3}-decay of the background also indicates the existence of one single domain within the irradiated volume in sample C.

From the averaged radial intensity profiles we find the characteristic spacings as listed in Table 2. The

Table 2. Measured q-values of the scattering in the columnar phase obtained from the radial profiles of the SAXS patterns and the inter- and intra-columnar spacings a_D, respectively, a_L, as calculated from the q-values.

Sample	$q_{(100)}/\mathrm{nm}^{-1}$	$q_{(110)}/\mathrm{nm}^{-1}$	$q_{(200)}/\mathrm{nm}^{-1}$	$q_{(210)}/\mathrm{nm}^{-1}$	$q_{(001)}/\mathrm{nm}^{-1}$
A	0.0282	0.0486	0.0561	0.0745	0.25
B	0.0281	0.0482	0.0551	0.0741	–
C	0.0272	0.0470	0.0541	0.0717	–
	a_D/nm				a_L/nm
A	257	259	259	258	25
B	258	261	263	259	–
C	267	267	268	268	–

inter-columnar spacings are calculated using the relation $a_D = \frac{4}{3}\sqrt{3}\sqrt{h^2+hk+k^2}/q_{(hk0)}$, while the average intra-columnar distance between the platelets is defined as $a_L = 2\pi/q_{(001)}$. Although samples A and B differ in overall platelet volume fraction, due to the first-order character of the nematic-columnar transition, the volume fractions of their columnar phases are the same. This explains their corresponding a_D. Sample C, on the other hand, contains non-adsorbing polymer, which enhances size fractionation between the coexisting phases [59,60], resulting in a higher average particle diameter in the columnar phase and hence a larger columnar spacing.

The formation of columnar crystals in our samples is actually quite surprising, considering the high polydispersity of our platelets. In general, phase-separating colloidal systems, of spheres [46,61–63] or platelets [59,60,64,65], deal with this by fractionation of the particles between the phases, leading to sub-phases with a (slightly) smaller polydispersity than the parent suspension. In sample C, where non-adsorbing polymer enhances fractionation even more, this lowering of the polydispersity facilitates the formation of the single columnar crystal. In addition to phase fractionation, there is the possibility of local fractionation, which is likely to take place in sample A due to its being a powder. Local fractionation leads to crystals within the columnar phase having a different average particle diameter (hence slightly different periods) and a slightly lower polydispersity each. However, in sample C, which contains a (large) single domain, such local fractionation is much more difficult as it would require the particles to travel too large distances (at least 1000 times their own diameter).

The $q_{(hk0)}$-values for samples A, B, and C correspond to nearest-neighbour distances of 258 nm, 260 nm, and 268 nm, respectively. From the histogram (of the parent suspension) it is immediately clear that at least 21% of the particles do not fit into a columnar phase with these spacings. For sample C, where size fractionation is strongest, the average particle diameter is larger than the parent's average, making accommodation of the particles in the columnar phase even more difficult.

4 Conclusions

To summarise, in this work we present clear evidence of the formation of hexagonal columnar liquid crystals in suspensions of polydisperse hard colloidal platelets. Apart from a powder of small columnar crystals, we find macroscopically large single-domain crystals. Our results suggest that addition of non-adsorbing polymer promotes the formation of single-domain crystals with unique orientation and no sign of disordered areas, as we have observed before in a suspension of hard colloidal spheres [55]. The macroscopically large crystals open up possibilities to fabricate nanostructured materials with a sub-micron periodicity that are of potential interest as, *e.g.*, photonic materials.

The authors thank Patrick Davidson for enlightening discussions. Igor Dolbnya and the other crew at the BM-26 DUBBLE-beamline (ESRF, Grenoble) are kindly thanked for their assistance during the measurements. The work of SMO is part of the SoftLink research programme of the "Stichting voor Fundamenteel Onderzoek der Materie (FOM)", which is financially supported by the "Nederlandse Organisatie voor Wetenschappelijk Onderzoek (NWO)".

References

1. P.N. Pusey, W. van Megen, Nature **320**, 340 (1986).
2. A. Imhof, D.J. Pine, Nature **389**, 948 (1997).
3. J.E.G.J. Wijnhoven, W.L. Vos, Science **281**, 802 (1998).
4. A. Blanco, E. Chomski, S. Grabtchak, M. Ibisate, S. John, S.W. Leonard, C. Lopez, F. Meseguer, H. Miguez, J.P. Mondia, G.A. Ozin, O. Toader, H.M. van Driel, Nature **405**, 437 (2000).
5. H. Zocher, Z. Anorg. Chem. **147**, 91 (1925).
6. F.C. Bawden, N.W. Pirie, J.D. Bernal, I. Fankuchen, Nature **138**, 1051 (1936).
7. L. Onsager, Phys. Rev. **62**, 558 (1942); Ann. N. Y. Acad. Sci. **51**, 627 (1949).
8. G. Oster, J. Gen. Physiol. **33**, 445 (1950).
9. U. Kreibig, C. Wetter, Z. Naturforsch. C **35**, 750 (1980).
10. J. Lapointe, D.A. Marvin, Mol. Cryst. Liq. Cryst. **19**, 269 (1973).
11. F.P. Booy, A.G. Fowler, Int. J. Biol. Macromol. **7**, 327 (1985).
12. Z. Dogic, S. Fraden, Phys. Rev. Lett. **78**, 2417 (1997).
13. Y. Maeda, S. Hachisu, Colloids Surf. **6**, 1 (1983); **7**, 357 (1983).
14. M. Wadati, A. Isihara, Mol. Cryst. Liq. Cryst. **17**, 95 (1972).
15. M. Hosino, H. Nakano, H. Kimura, J. Phys. Soc. Jpn. **46**, 1709 (1979); **47**, 740 (1979); **51**, 741 (1982).
16. B. Mulder, Phys. Rev. A **35**, 3095 (1987).
17. X. Wen, R.B. Meyer, Phys. Rev. Lett. **59**, 1325 (1987).

18. A. Poniewierski, R. Holyst, Phys. Rev. Lett. **61**, 2461 (1988).
19. A. Stroobants, H.N.W. Lekkerkerker, D. Frenkel, Phys. Rev. Lett. **57**, 1452 (1986); Phys. Rev. A **36**, 2929 (1987).
20. D. Frenkel, H.N.W. Lekkerkerker, A. Stroobants, Nature **332**, 822 (1988).
21. I. Langmuir, J. Chem. Phys. **6**, 873 (1938).
22. A. Mourchid, A. Delville, J. Lambard, E. Lécolier, P. Levitz, Langmuir **11**, 1942 (1995).
23. M. Kroon, G.H. Wegdam, R. Sprik, Phys. Rev. E **54**, 6541 (1996).
24. A. Mourchid, E. Lécolier, H. Van Damme, P. Levitz, Langmuir **14**, 4718 (1998).
25. P. Levitz, E. Lécolier, A. Mourchid, A. Delville, S. Lyonnard, Europhys. Lett. **49**, 672 (2000).
26. J.C.P. Gabriel, C. Sanchez, P. Davidson, J. Phys. Chem. **100**, 11139 (1996).
27. H. van Olphen, J. Colloid Interface Sci. **19**, 313 (1964).
28. E. Lécolier, A. Mourchid, P. Levitz, Prog. Colloid Polym. Sci. **110**, 16 (1998).
29. P.F. Luckham, S. Rossi, Adv. Colloid Interface Sci. **89**, 43 (1999).
30. J.D.F. Ramsay, S.W. Swanton, J. Bunce, J. Chem. Soc. Faraday Trans. **86**, 3919 (1990).
31. J.D.F. Ramsay, P. Lindner, J. Chem. Soc. Faraday Trans. **89**, 4207 (1993).
32. F. Pignon, J.M. Piau, A. Magnin, Phys. Rev. Lett. **76**, 4857 (1996).
33. B.J. Lemaire, P. Panine, J.C.P. Gabriel, P. Davidson, Europhys. Lett. **59**, 55 (2002).
34. F.M. van der Kooij, H.N.W. Lekkerkerker, J. Phys. Chem. B **102**, 7829 (1998).
35. D. van der Beek, H.N.W. Lekkerkerker, Europhys. Lett. **61**, 702 (2003).
36. D. Frenkel, R. Eppenga, Phys. Rev. Lett. **49**, 1089 (1982).
37. J.A.C. Veerman, D. Frenkel, Phys. Rev. A **45**, 5632 (1992).
38. S.-D. Zhang, P.A. Reynolds, J.S. van Duijneveldt, J. Chem. Phys. **117**, 9947 (2002).
39. F.M. van der Kooij, K. Kassapidou, H.N.W. Lekkerkerker, Nature **406**, 868 (2000).
40. A.B.D. Brown, S.M. Clarke, A.R. Rennie, Langmuir **14**, 3129 (1998).
41. D. van der Beek, H.N.W. Lekkerkerker, Langmuir **20**, 8582 (2004).
42. J.L. Barrat, J.P. Hansen, J. Phys. (Paris) **46**, 1547 (1986).
43. P.N. Pusey, J. Phys. (Paris) **48**, 709 (1987).
44. R. McRae, A.D.J. Haymet, J. Chem. Phys. **88**, 1114 (1988).
45. P.N. Pusey, in *Liquids, Freezing and Glass Transition*, Les Houches Session 51, NATO Advanced Study Institute, Series B: Physics, edited by J.P. Hansen, D. Levesque, J. Zinn-Justin (North-Holland, Amsterdam, 1991) pp. 763.
46. P.G. Bolhuis, D.A. Kofke, Phys. Rev. E **54**, 634 (1996).
47. J. Torbet, G. Maret, J. Mol. Biol. **134**, 843 (1979).
48. E. Senechal, G. Maret, K. Dransfeld, Int. J. Biol. Macromol. **2**, 256 (1980).
49. J. Torbet, J.M. Freyssinet, G. Hudry-Clergeon, Nature **289**, 91 (1981).
50. J.M. Freyssinet, J. Torbet, G. Hudry-Clergeon, G. Maret, Proc. Natl. Acad. Sci. USA **80**, 1616 (1983).
51. R. Oldenbourg, X. Wen, R.B. Meyer, D.L.D. Caspar, Phys. Rev. Lett. **61**, 1851 (1988).
52. J. Gregory, K.C. Holmes, J. Mol. Biol. **13**, 796 (1965).
53. M. Impéror-Clerc, P. Davidson, Eur. Phys. J. B **9**, 93 (1999).
54. A.B.D. Brown, A.R. Rennie, Phys. Rev. E **62**, 851 (2000).
55. A.V. Petukhov, D.G.A.L. Aarts, I.P. Dolbnya, E.H.A. de Hoog, K. Kassapidou, G.J. Vroege, W. Bras, H.N.W. Lekkerkerker, Phys. Rev. Lett. **88**, 208301 (2002).
56. A.V. Petukhov, I.P. Dolbnya, D.G.A.L. Aarts, G.J. Vroege, H.N.W. Lekkerkerker, Phys. Rev. Lett. **90**, 028304 (2003).
57. A.V. Petukhov, I.P. Dolbnya, D.G.A.L. Aarts, G.J. Vroege, Phys. Rev. E **69**, 031405 (2004).
58. A.M. Wierenga, T.A.J. Lenstra, A.P. Philipse, Colloids Surf. A **134**, 359 (1998).
59. F.M. van der Kooij, M. Vogel, H.N.W. Lekkerkerker, Phys. Rev. E **62**, 5397 (2000).
60. F.M. van der Kooij, H.N.W. Lekkerkerker, Langmuir **16**, 10144 (2000).
61. D.A. Kofke, P.G. Bolhuis, Phys. Rev. E **59**, 618 (1999).
62. S.R. Williams, I.K. Snook, W. van Megen, Phys. Rev. E **64**, 021506 (2001).
63. N.B. Wilding, P. Sollich, Europhys. Lett. **67**, 219 (2004).
64. M.A. Bates, D. Frenkel, J. Chem. Phys. **110**, 6553 (1999).
65. F.M. van der Kooij, H.N.W. Lekkerkerker, Phys. Rev. Lett. **84**, 781 (2000).